eXPRESS Polymer Letters Vol.7, No.6 (2013) 495–504
Available online at www.expresspolymlett.com
DOI: 10.3144/expresspolymlett.2013.46

Synthesis and characterization of an electrolyte system based on a biodegradable polymer

K. Sownthari[*], *S. A. Suthanthiraraj*

Department of Energy, University of Madras, Guindy (Maraimalai) Campus, 600025 Chennai, India

Received 26 November 2012; accepted in revised form 16 February 2013

Abstract. A polymer electrolyte system has been developed using a biodegradable polymer namely poly-ε-caprolactone (PCL) in combination with zinc triflate [$Zn(CF_3SO_3)_2$] in different weight percentages and characterized during this investigation. Free-standing thin films of varying compositions were prepared by solution casting technique. The successful doping of the polymer has been confirmed by means of Fourier transform infrared spectroscopy (FTIR) by analyzing the carbonyl (C=O) stretching region of the polymer. The maximum ionic conductivity obtained at room temperature (25°C) was found to be 8.8×10^{-6} S/cm in the case of PCL complexed with 25 wt% $Zn(CF_3SO_3)_2$ which is five orders of magnitude higher than that of the pure polymer host material. The increase in amorphous phase with an increase in salt concentration of the prepared polymer electrolyte has also been confirmed from the concordant results obtained from X-ray diffraction (XRD), differential scanning calorimetry (DSC) and scanning electron microscopic (SEM) analyses. Furthermore, the electrochemical stability window of the prepared polymer electrolyte was found to be 3.7 V. An electrochemical cell has been fabricated based on Zn/MnO_2 electrode couple as an application area and its discharge characteristics were evaluated.

Keywords: *biodegradable polymers, conductivity, zinc triflate, polymer electrolyte*

1. Introduction

Owing to the fact that the field of polymers has a wide range of applications compared to any other class of materials available to mankind, polymer industry has grown up more rapidly than any other industry in recent years. Their applications extend from adhesives, coatings, packaging to precursors for high-tech ceramics. The first potential use of polymer as an electrolyte material was examined by Wright and Armand in 1970s which paved the growth of a new area of research called 'Polymer electrolytes'. Polymer electrolytes are essentially polymer-salt complexes formed by dissolving salts in a polymer matrix containing heteroatoms such as O, N, S, etc.

Polymer electrolytes are known to exhibit several advantages like flexibility, ease of thin film formation and good mechanical stability over liquid electrolytes which are deemed to be hazardous as they may leak, produce undesirable gases on overcharging and even explode. Even though battery technology was developed one hundred years ago, the search for new materials possessing better performance, high energy density and extended cycles of rechargeability has only been the main subject of considerable attention, whereas the use of non-toxic and non-hazardous surrogate materials has not yet been systematically developed [1].

Most of the experimental research work on polymer electrolytes carried out towards development of lithium polymer batteries was based on poly (ethylene oxide) (PEO) with various inorganic salts dissolved within its matrix. A few attempts have already been made on biodegradable natural polymers such

[*]Corresponding author, e-mail: sownthari@gmail.com

as cellulose acetate (CA) [2], starch [3], gelatin [4] and chitosan [5] and biodegradable synthetic polymer such as poly (vinyl alcohol) (PVA) [6] which are being used as polymer hosts for obtaining new polymer electrolytes for their applications in various electrochemical devices such as batteries, sensors and electrochromic windows.

It is worthwhile to mention that poly-ε-caprolactone (PCL) is a linear aliphatic semicrystalline thermoplastic polyester having a low melting point of around 60°C and a glass transition temperature of about –60°C which may be completely degraded in the presence of microbes or aqueous medium by the hydrolysis of ester bonds [7] and its mechanical property is good as well. As a consequence, PCL is now enjoying a wide range of application from packaging to biomedical implants [8]. A very few researchers have attempted to fabricate compostable battery systems using biodegradable polymer electrolyte with PCL as polymer host [9–13].

Although lithium ion battery has several advantages, safety and environmental issues associated with lithium ion battery cannot be ignored [14]. Zinc would be a good alternative for lithium since the sizes of Li^+ and Zn^{2+} ions are comparable and safety problems associated with zinc are minimal and hence may be handled easily. From the literature survey it is quite evident that studies on solid polymer electrolytes related to zinc batteries are scanty [15–18].

Thus in this paper, the biodegradable polymer PCL has been used to prepare a new series of zinc ion conducting polymer electrolytes in order to replace traditional polymer electrolytes which are more harmful to the environment.

2. Experimental

2.1. Materials and method

PCL with M_n = 80 kDa and zinc trifluoromethanesulfonate $Zn(CF_3SO_3)_2$ (zinc triflate, ZnTr) with M_w = 363.53 g/mol were procured from Sigma-Aldrich, USA. ZnTr was dried at 100°C for an hour prior to use as the incorporating salt, while PCL was used, as received. Zinc ion conducting polymer electrolytes consisting of PCL complexed with ZnTr in various composition were prepared by solution casting technique. Appropriate amounts of polymer and salt with various PCL:ZnTr ratio in wt% were dissolved in a common solvent namely tetrahydrofuran (THF). The mixtures were stirred continuously for several hours at room temperature in order to obtain homogenous viscous solutions. Such solutions were then cast into different glass petri dishes and maintained at 50°C for THF to evaporate and then vacuum dried at 50°C for 15 h. The films were further dried slowly at room temperature inside a desiccator for 2 days to remove any traces of solvent. Self-standing translucent films were obtained up to 25 wt% loading of salt, beyond which the films were no longer mechanically stable. The average thickness of the films measured by air wedge technique was around 60–70 μm.

2.2. Characterizations

FTIR spectroscopy has been employed to investigate molecular level interactions occurring between the polymer-host and salt system. The spectra were recorded on neat film in the transmission mode at room temperature using a Perkin-Elmer RX1 spectrophotometer with a wavenumber resolution of 4 cm^{-1} over the wavenumber range 4000–500 cm^{-1}. AC impedance measurements were carried out in the frequency range 1 MHz–20 Hz with an excitation signal of 500 mV using a computer-controlled Hewlett-Packard Model HP 4284A Precision LCR Meter in the temperature window 25–50°C. The polymer electrolyte films were sandwiched between two polished stainless steel (SS) disks and such symmetrical cells involving blocking interfaces with the configuration – [SS/polymer electrolyte/SS] were used for impedance measurements.

X-ray diffraction measurements were performed using a Bruker D8 Advance diffractometer equipped with monochromatic Cu K_α radiation (λ = 1.54 Å) at 40 kV and 30 mA with a step size of 0.1° from 10–80° at room temperature. Thermal behavior of the polymer electrolytes was analyzed using a differential scanning calorimeter by using NETZSCH DSC 204. The samples were heated in closed aluminum pans under nitrogen atmosphere to 90°C, cooled to –90°C and then heated to 90°C at a heating rate of 10°C/min. The thermograms corresponding to second heating were recorded and used for analysis.

Surface morphology of the samples was characterized at room temperature by means of a Hitachi S-3400 model scanning electron microscope at 15 kV. The samples were coated with a thin layer of gold by vacuum sputtering for 20 s in order to prevent electrostatic charging.

The electrochemical stability window of the prepared polymer electrolyte was determined by linear sweep voltammetry (LSV) employing inert stainless steel disc as working electrode and zinc metal plate as reference and counter electrodes. The Zn/polymer electrolyte/SS cell was constructed and utilized at a scan rate of 10 mV/s from 0 to 5 V vs. Zn/Zn^{2+}. The reversibility of Zn plating/stripping at room temperature has been verified by cyclic voltammetry at a scan rate of 10 mV/s using the symmetric Zn/polymer electrolyte/Zn cell configuration from -1.5 to +1.5 V. Prototype Zn|polymer electrolyte|MnO_2 cell has also been fabricated based on the prepared polymer electrolyte and its discharge characteristics has been tested.

2.3. Preparation of Zn|polymer electrolyte|MnO_2 cell

The manganese dioxide cathode was prepared using battery grade γ-MnO_2 (electrolytic manganese dioxide, EMD). A mixture of EMD (80 wt%), graphite powder (10 wt%) and polymer electrolyte (10 wt%) as a binder was taken in a mortar and ground together along with a small amount of acetone and then the slurry was applied onto a nickel grid. The nickel grid was subjected to degreasing in NaOH solution and etching in dilute HCl, prior to use. The nickel grid along with the slurry was heated at 80°C for about 5 min and then pressed at a pressure of 250 MPa. Polymer electrolyte film was sandwiched between this MnO_2 cathode and zinc foil. The open-circuit voltage was measured without any load, and short circuit current was measured when the cell was short-circuited whereas, the discharge characteristics of the cell were monitored under a constant load of 1 MΩ with the aid of a digital voltmeter and ammeter, connected parallel and in series to the load, respectively.

3. Results and discussion

In this study, FTIR spectroscopy has been used to confirm the coordination or the complexation of the dopant salt with the host polymer. Figure 1 shows the FTIR spectra recorded at room temperature in the case of PCL:ZnTr complexes with various weight ratios.

In the case of pure polymer PCL, the carbonyl (C=O) group absorption region appears at 1800–1650 cm^{-1} and is highly sensitive to ionic interactions. Since the carbonyl group is a strong electron donor within this polyester-based polymer electrolyte, zinc ion tends to coordinate with oxygen atom of carbonyl group [19]. In addition to a peak at 1720 cm^{-1} for pure PCL, a shoulder peak at around 1650 cm^{-1} appears upon addition of salt and grows on increasing the salt concentration as shown in Figure 2 which confirms the formation of PCL:ZnTr complex or the successful doping of the biodegradable polymer, PCL.

In general, on dissolution of salt into polymer, oxygen atom of triflate remains uncoordinated or either coordinated with Zn^{2+}. While coordinating with Zn^{2+} ion, the asymmetric stretching of SO_3 seen at 1274 cm^{-1} corresponding to the free triflate, splits

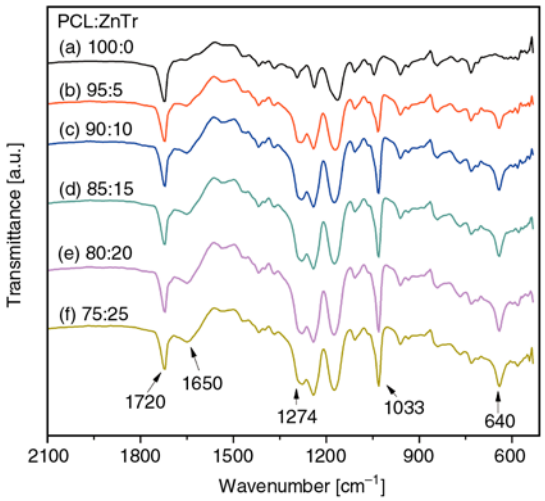

Figure 1. FTIR spectra recorded at room temperature for PCL:ZnTr complexes with various compositions

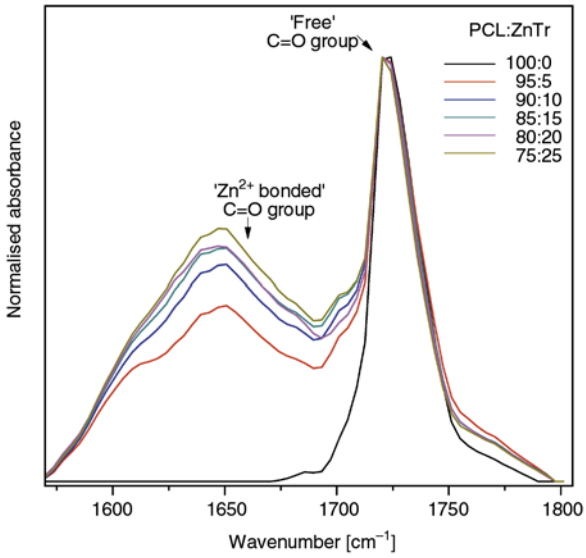

Figure 2. The C=O stretching region of PCL:ZnTr complex with different compositions showing the growth of a shoulder peak at 1650 cm^{-1} corresponding to Zn^{2+} ion interaction

into two components at 1313 and 1241 cm^{-1} [20]. Thus, the overlapping complex spectra in the region 1350–1200 cm^{-1} implies the presence of contact ion pair and ion aggregates in addition to free triflate ions even at lower concentration of salt. A peak at 1033 cm^{-1} is observed in all the spectra of polymer-salt complexes and it is attributable to the symmetric stretching vibration mode of SO_3 which come from free triflate ions [21]. Since the area under peak is representative of abundance of that particular entity, the observed increase in peak intensity and area at 1033 cm^{-1} with progressive addition of salt from 0 to 25 wt% directly indicates an increase in the number of free triflate ions as shown in Figure 3. The peak at 640 cm^{-1} corresponding to the bending of CF_3 and SO_3 groups and CS symmetrical stretching also increases with the increase in the salt concentration thus confirming the above fact. In addition, characteristic peaks of PCL are observed at 1172, 1238, 1292, 1165, 1190 and 960 cm^{-1} corresponding to symmetric and asymmetric COC stretching, C–O and C–C stretching in crystalline and amorphous phases, OC–O stretching and CH_2 rocking respectively.

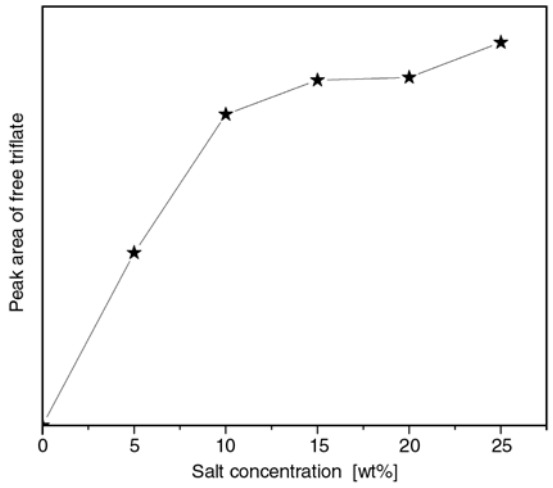

Figure 3. Area under the peak at 1033 cm^{-1} owing to free triflate ion as a function of salt concentration over the range 0 to 25 wt%

Nyquist plots of PCL incorporated with different concentrations of ZnTr at room temperature are shown in Figure 4a and 4b.

Nyquist plot of each sample shows two well defined regions. The high frequency semicircle represents the relaxation process associated with the bulk of the polymer electrolyte which can be viewed into a parallel combination of bulk resistance and bulk capacitance arising from the migration of ions and immobile polymer chains polarized by the applied field respectively. The centre of the semicircle is displaced below the *x*-axis with more than one relaxation time of the ions in the polymer electrolyte. The low frequency spike represents the built-up of charges resulting from the polarization at the electrode/electrolyte interface and is supposed to be parallel to the imaginary axis, but in this case, the spike is found to be inclined making an angle with the imaginary axis and is related to the double layer formation at the blocking electrodes [22].

From the literature survey, the conductivity of the pure PCL at room temperature is found to be 1.86×10^{-11} S/cm [10]. The conductivity of PCL-ZnTr complex increases to 2.3×10^{-8} upon a addition of 5 wt% of the salt and it is observed that the value of conductivity increases with the increase of salt content and reaches a maximum of 8.8×10^{-6} S/cm

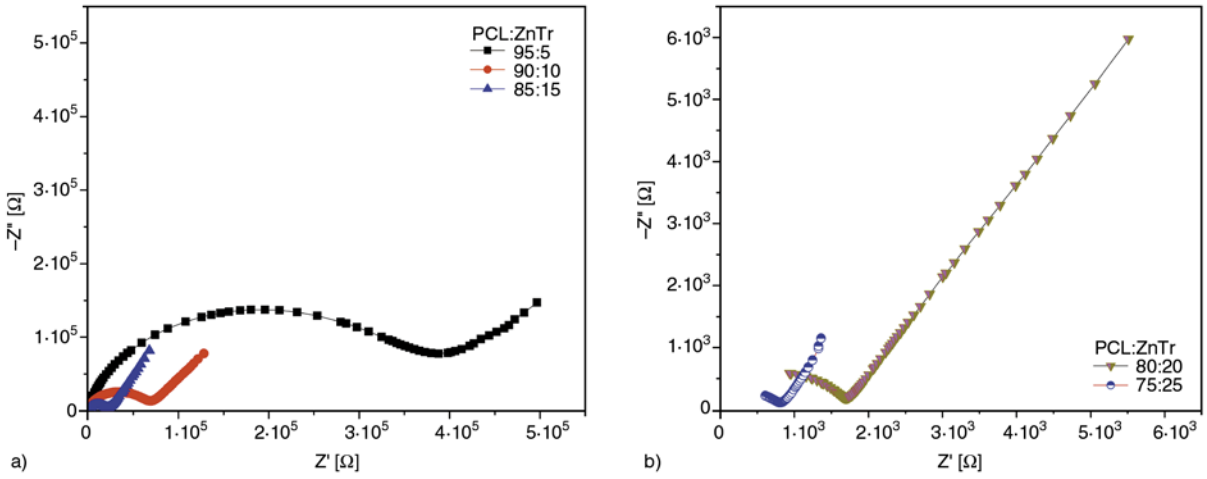

Figure 4. Nyquist plots obtained at room temperature for the complex PCL:ZnTr with (a) 5, 10 and 15; (b) 20 and 25 wt% loading of the salt

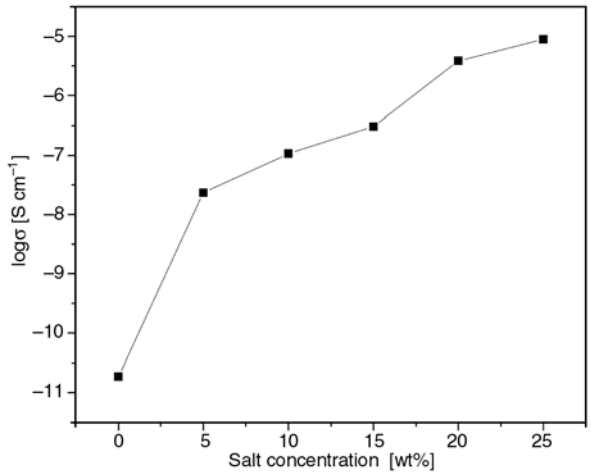

Figure 5. Variation of ionic conductivity with respect to salt concentration in the region 0 to 25 wt% at room temperature (25°C)

for 25 wt% loading of the salt which is five orders of magnitude higher than that of the reported value of conductivity of pure PCL. A plot of variation of ionic conductivity against salt concentration is given in Figure 5 showing the increasing trend in the value of conductivity of the PCL-ZnTr complex with increase in the salt content at room temperature (25°C).

The salt concentration dependence of dielectric constant (ε') at different frequencies is plotted in Figure 6. Since the dielectric constant is a direct measure of the number density of ions, the increase in the dielectric constant values may be related to the increase in the number of charge carriers available for conduction [13]. With the increase in the

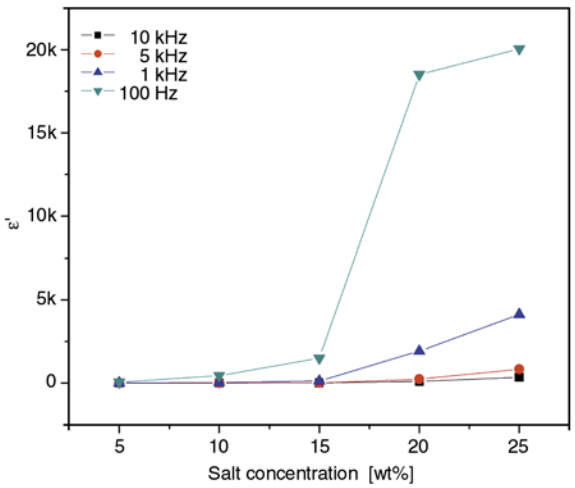

Figure 6. Variation of dielectric constant with respect to salt concentration at four different frequencies of measurement namely 10, 5, 1 kHz and 100 Hz repectively

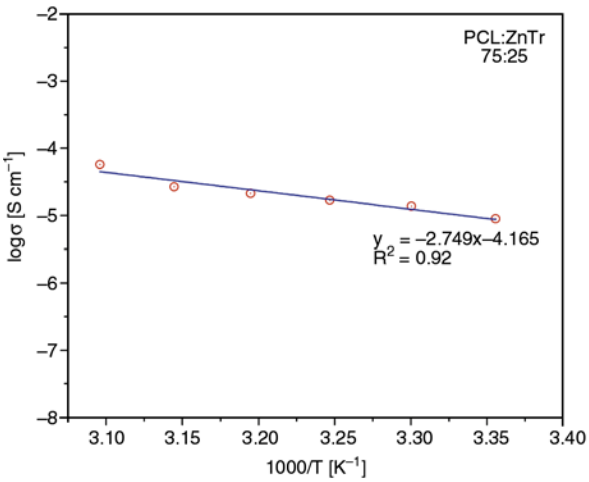

Figure 7. Ionic conductivity as a function of temperature for PCL:ZnTr with 25 wt% loading of the salt

frequency of measurement, ε' is found to decrease and this aspect may be due to the fact that the periodic reversal of the applied field is so rapid that Zn^{2+} ions could not diffuse in the direction of the electric field and hence could not contribute to the increase in the value of the dielectric constant. It is also found that the observed dielectric constant increases with increase of salt concentration and hence the number of ions for conduction increases as confirmed from the present FTIR studies.

Figure 7 shows the linear dependence of logarithm of ionic conductivity of PCL:ZnTr complex with 25 wt% loading of the salt on inverse of temperature and follows an Arrhenius-type thermally activated process. Hence, it may be inferred that Zn^{2+} ions are transported via the hopping mechanism which could be explained on the basis of Equation (1):

$$\sigma = \sigma_0 \exp\left(-\frac{E_a}{kT}\right) \quad (1)$$

where σ_0 is the pre-exponential factor, E_a the activation energy, k the Boltzmann constant and T is the temperature. The activation energy (E_a) has been calculated by considering the slope after linear fitting the data and is found to be 0.54 eV.

Figure 8 depicts the room temperature XRD patterns of PCL:ZnTr complexes with different weight ratios. The XRD pattern of pure PCL illustrates three strong diffraction peaks at $2\theta = 21.4$, 22 and 23.7° which correspond to the orthorhombic [23] planes (110), (111) and (200) and a halo centered at 21° indicating that the film is semicrystalline comprising both crystalline and amorphous phases.

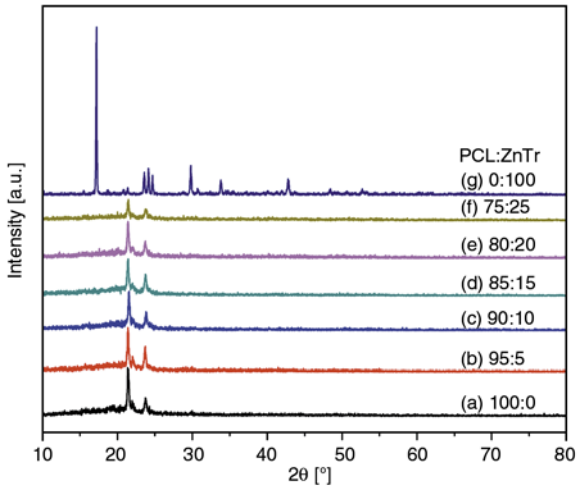

Figure 8. XRD patterns of different compositions of PCL:ZnTr complexes

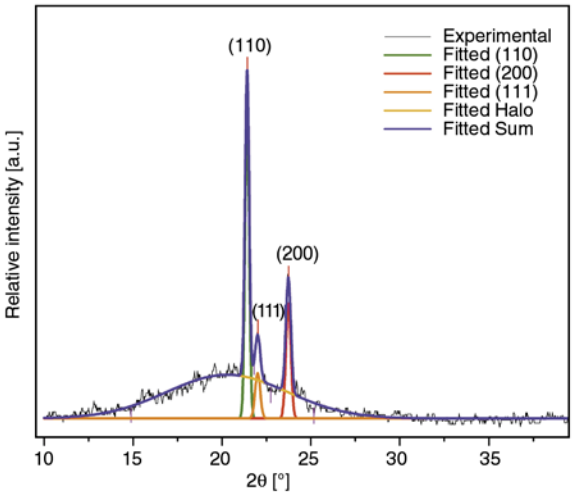

Figure 9. Deconvoluted XRD pattern of pure PCL showing Gaussian fittings of (110), (111), (200) and halo

Upon addition of ZnTr salt, the intensity of diffraction peaks corresponding to the crystalline phases decrease due to the transformation of crystalline into amorphous phases thus indicating the complexation of salt and polymer. Since the conductivity is supported by the amorphous phase of the polymer electrolyte, the result inferred from XRD is in good agreement with the conductivity measurements. The average crystallite size of the polymer complexes has been calculated from the full-width-half-maximum (FWHM) using the Scherrer's formula (Equation (2)):

$$C = 0.94\frac{\lambda}{\beta\cos\theta} \tag{2}$$

where λ is the wavelength of the X-ray used which is 1.5406 Å, β the FWHM of the peak and θ is the Bragg diffraction angle. The average crystallite size of the nanocrystals is found to be in the range of 42.6–30 nm. The fact that, no peaks corresponding to the salt are seen in the XRD patterns of PCL:ZnTr complexes tends to confirm the complete dissolution of the salt into the chosen polymer matrix [13].

The crystallinity of the sample has been calculated by deconvoluting peaks due to amorphous and crystalline phases on diffraction pattern [24] using peak separation software Origin Pro 8 and according to Equation (3):

$$\chi_c = \frac{I_c}{I_c + I_a} \tag{3}$$

where I_c represents the total crystalline area under 21.4, 22 and 23.7° and I_a represents amorphous area under the halo at 21°. The deconvoluted XRD pattern of pure PCL is shown in Figure 9. The calculated value of degree of crystallinity is found to decrease from 44.3 to 27.8% while increasing the ZnTr salt content from 0 to 25%.

Thermograms of PCL:ZnTr complexes with different weight ratios are given in Figure 10. Pure PCL showed a phase transition at –63.3°C, which is attributed to the glass transition temperature (T_g). The backbone chain of PCL exhibits a higher flexibility characterized by a low glass transition temperature [25] and requires low activation energy to allow any conformational changes within the polymer, satisfying the basic criteria to use a polymer as a host material to prepare polymer electrolytes. Upon addition of ZnTr salt, the interaction of salt with polymer hinders bond rotation and therefore, stiffens the polymer chain thereby increasing the

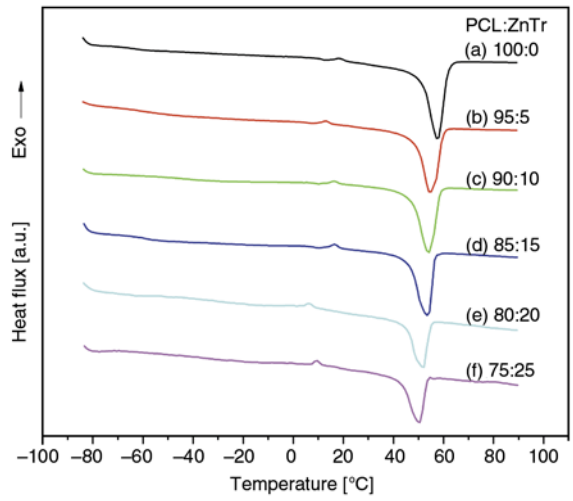

Figure 10. DSC thermograms of different compositions of PCL:ZnTr complexes

value of T_g to a maximum of –57.3 for 25 wt% loading of salt.

In the case of pure polymer, a sharp endotherm observed at 55.3°C may be attributed to the melting of crystalline phase of relatively larger spherulites associated with the semicrystalline polymer. With the addition of 5 wt% of salt, the melting peak shifts to 54.7°C which is due to the complexation occurring between the salt and polymer. With further increase of salt content within the polymer electrolyte, the melting peak shifts towards lower temperature and reaches a minimum of 50.6°C for 25 wt% loading of salt may be due to the increase in the percentage of complexation between the polymer and salt as confirmed by analyzing the carbonyl stretching region of FTIR spectra which in turn increases the disorder of the crystalline phases. The enthalpy of melting of the polymer complexes decreases with the progressive increase of salt content and is a confirmation of increase in the amorphous phase or disorder within the crystalline phase of the polymer electrolyte. The relative degree of crystallinity has been calculated as the ratio of enthalpy of fusion of polymer electrolyte (ΔH_m) to enthalpy of fusion of hypothetical crystal of of PCL (ΔH^0_{PCL}). From the literature, the value of ΔH^0_{PCL} is found to be 136 J/g [26]. The degree of crystallinity is found to decrease from 45.2 to 31% while increasing the salt content from 0 to 25%. In all the samples, the degree of crystallinity calculated from DSC is slightly greater than that of the crystallinity calculated from XRD due to the possibility of recrystallization during DSC measurements [27].

All the prepared samples were analyzed using scanning electron microscopy (SEM) in order to study the surface morphology of these polymer electrolytes. Figure 11a-c shows the SEM images of the PCL:ZnTr complex for 0, 15, 25 wt% loading of the salt. It is interesting to note that pure PCL polymer film exhibits the spherulite texture with individual spherulite sizes in several thousands of micrometer in diameter with spherulites occurring via sporadical nucleation and growing radially until they impose upon each other at straight boundaries [28] as can be seen from Figure 11a which is a characteristic of a semi-crystalline polymer. The surface of the film is comparatively rough with spherulites closely packed with each other. Upon addition of salt the spherulite size significantly reduces with the increase in the number of spherulites. On further increase in the amount of salt content in the polymer-salt complex, the surface becomes smoother with the appearance of amorphous phases and boundaries become clearly visible. It is also found that in the case of the best

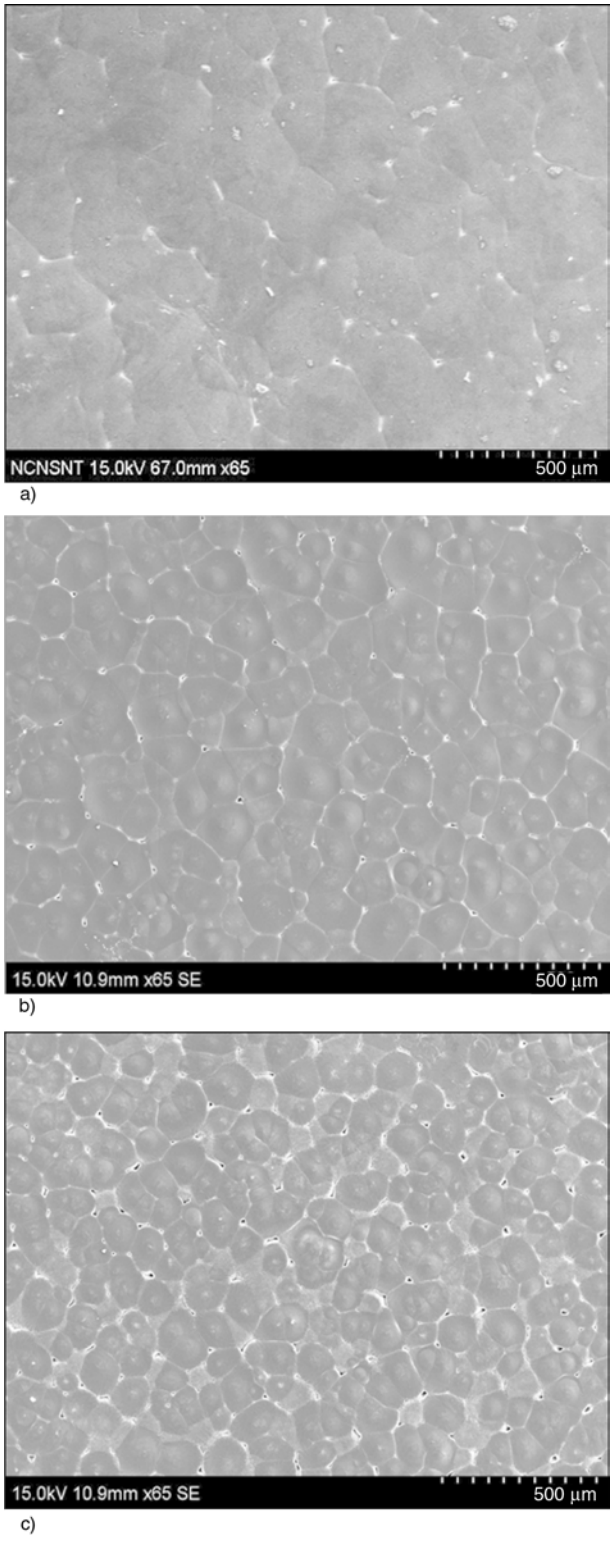

Figure 11. SEM images of PCL:ZnTr complex in (a) 100:0; (b) 85:15 and (c) 75:25 weight ratios

conducting complex, PCL:ZnTr 75:25 wt%, the smoother portion increases much more and favors ionic conduction.

From the application point of view, determination of electrochemical stability window of an electrolyte where no oxidation/reduction takes place within the polymer electrolyte system is essential for fabricating an electrochemical device. In this regard, the stability window of the highly conducting complex, 75:25 wt% PCL:ZnTr was experimentally determined using linear sweep voltammetry. From the voltammogram shown in Figure 12, anodic current was negligible below +2.7 V and when the voltage crosses +2.7 V, the anodic current begins to flow and increases gradually. For $(PEO)_8LiClO_4$ system, Scrosati [29] attributed this anodic current with the oxidation of anion followed by the degradation of the polymer chains by the attack of hydrogen. Therefore, in the present system also, the triflate oxidation and polymeric degradation may take place in the higher voltage region (above +2.7 V) according to the following reactions:

$$CF_3SO_3^- \longrightarrow CF_3SO_3^{\bullet} + e^- \quad \text{(triflate oxidation)}$$

$$CF_3SO_3^{\bullet} + H\text{–}\underset{|}{\overset{|}{C}}\text{–} \longrightarrow CF_3SO_3H + {}^{\bullet}\underset{|}{\overset{|}{C}}\text{–}$$

(polymeric degardation)

The upper limit of the electrolyte stability was generally taken to be the point of intersection obtained by extrapolating the higher voltage linear current with the *x*-axis [30] which is found to be 3.7 V for the present case, which is fair enough to construct a zinc primary as well as rechargeable battery based on Zn^{2+} intercalating/deintercalating γ-MnO_2 electrode, since γ-MnO_2 is an extensively used electrode to intercalate/deintercalate Zn^{2+} in liquid electrolyte-based rechargeable batteries [31].

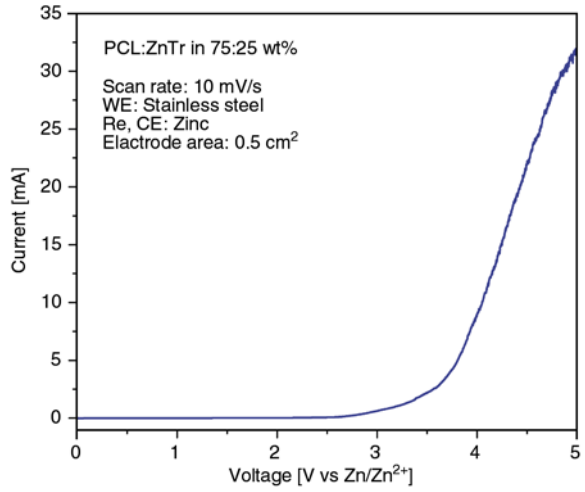

Figure 12. Linear sweep voltammogram of 75:25 wt% PCL:ZnTr complex employing Zn/Polymer Electrolyte/SS cell at 25°C

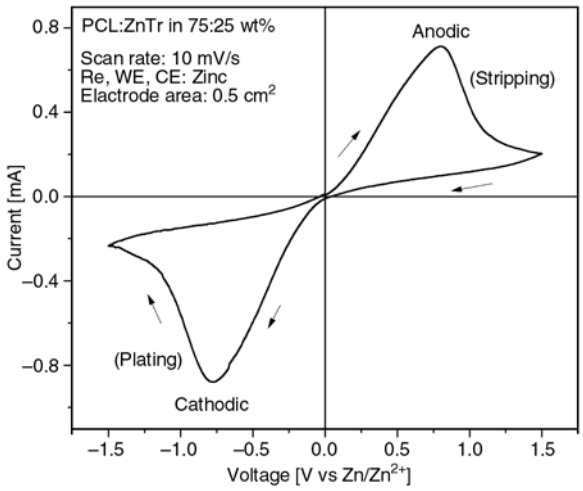

Figure 13. Cyclic voltammogram recorded for 75:25 wt% PCL:ZnTr complex showing the zinc plating/stripping process of Zn/Polymer Electrolyte/Zn cell at 25°C

Further, cyclic voltammetry was also carried out with a view to obtain an evidence of the zinc plating/stripping process. Cyclic voltammogram recorded in the case of 75:25 wt% PCL:ZnTr complex is shown in Figure 13, in which the ratio of anodic to cathodic peak current provided an yield of 82% at a scan rate of 10 mV/s. This reveals the possibility of dissolution of zinc into and deposition from polymer electrolyte during discharging and charging by the oxidation of zinc metal into Zn^{2+} and reduction of Zn^{2+} into Zn respectively as reported in other divalent cationic systems like Mg^{2+} [32].

The observed discharge characteristics in the case of the cell Zn|polymer electrolyte|MnO_2 at room temperature (25°C) for a constant load of 1 MΩ is shown in Figure 14. The open-circuit voltage and short-circuit current of the freshly prepared cell were found to be 1.6 V and 0.71 mA, respectively. Interestingly, the discharge voltage-time characteristics of the cell exhibited a stable and constant behavior with a plateau at ~1.4 V for about 100 h thus confirming the electrochemical compatibility and stability of the PCL:ZnTr complex as a polymer electrolyte system.

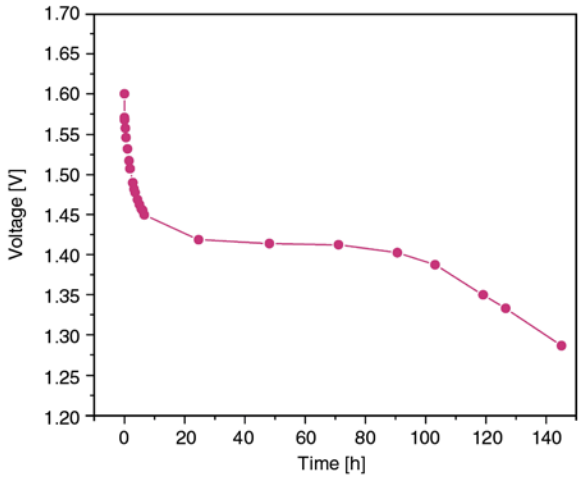

Figure 14. Discharge curve for the Zn|Polymer electrolyte|MnO_2 cell for a constant load of 1 MΩ at room temperature (25°C)

4. Conclusions

The possibility of developing a biodegradable polymer electrolyte based on PCL complexed with zinc triflate has been successfully demonstrated. The complexation between the salt and polymer was confirmed using FTIR studies. With the introduction of salt, the ionic conductivity of PCL was found to increase dramatically from 10^{-11} to 10^{-6} S/cm for 25 wt% loading of salt. The reduction in crystallinity has been confirmed from XRD analysis and further supported by DSC data whereas the rough surface of PCL becomes a smoother one due to the addition of salt as observed from SEM features. Additionally, the highly conducting composition exhibited an appreciably good elctrochemical stability window of 3.7 V with an excellent reversibility. A prototype electrochemical cell based on the Zn/MnO_2 electrode couple has also been fabricated and the cell showed stable and constant discharge characteristics at room temperature, thus indicating its practical applications.

Acknowledgements

The authors would like to thank NCNSNT, University of Madras for SEM analysis and DST for DSC analysis. One of the authors (K. S.) thanks DST, New Delhi for the financial support received in the form of INSPIRE fellowship.

References

[1] Abdullah M., Lenggoro W., Okuyama K.: Polymer electrolyte nanocomposites. in 'Encyclopedia of nanoscience and nanotechnology' (ed.: Nalwa H. S.), Vol 8, 731–762 (2004).

[2] Selvakumar M., Bhat D. K.: $LiClO_4$ doped cellulose acetate as biodegradable polymer electrolyte for supercapacitors. Journal of Applied Polymer Science, **110**, 594–602 (2008).
DOI: 10.1002/app.28671

[3] Ramesh S., Liew C-W., Arof A. K.: Ion conducting corn starch biopolymer electrolytes doped with ionic liquid 1-butyl-3-methylimidazolium hexafluorophosphate. Journal of Non-Crystalline Solids, **357**, 3654–3660 (2011).
DOI: 10.1016/j.jnoncrysol.2011.06.030

[4] Avellaneda C. O., Vieira D. F., Al-Kahlout A., Heusing S., Leite E. R., Pawlicka A., Aegerter M. A.: All solid-state electrochromic devices with gelatin-based electrolyte. Solar Energy Materials and Solar Cells, **92**, 228–233 (2008).
DOI: 10.1016/j.solmat.2007.02.025

[5] Puteh R., Yahya M. Z. A., Ali A. M. M., Sulaiman M. A., Yahya R.: Conductivity studies on chitosan-based polymer electrolytes with lithium salts. Indonesian Journal of Physics, **16**, 17–19 (2005).

[6] Malathi J., Kumaravadivel M., Brahmanandhan G. M., Hema M., Baskaran R., Selvasekarapandian S.: Structural, thermal and electrical properties of PVA–$LiCF_3SO_3$ polymer electrolyte. Journal of Non-Crystalline Solids, **356**, 2277–2281 (2010).
DOI: 10.1016/j.jnoncrysol.2010.08.011

[7] Khatiwala V. K., Shekhar N., Aggarwal S., Mandal U. K.: Biodegradation of poly(ε-caprolactone) (PCL) film by *Alcaligenes faecalis*. Journal of Polymers and the Environment, **16**, 61–67 (2008).
DOI: 10.1007/s10924-008-0104-9

[8] Wang Y., Rodriguez-Perez M. A., Reis R. L., Mano J. F.: Thermal and thermomechanical behaviour of polycaprolactone and starch/polycaprolactone blends for biomedical applications. Macromolecular Materials and Engineering, **290**, 792–801 (2005).
DOI: 10.1002/mame.200500003

[9] Fonseca C. P., Rosa D. S., Gaboardi F., Neves S.: Development of a biodegradable polymer electrolyte for rechargeable batteries. Journal of Power Sources, **155**, 381–384 (2006).
DOI: 10.1016/j.jpowsour.2005.05.004

[10] Woo H. J., Majid S. R., Arof A. K.: Conduction and thermal properties of a proton conducting polymer electrolyte based on poly (ε-caprolactone). Solid State Ionics, **199–200**, 14–20 (2011).
DOI: 10.1016/j.ssi.2011.07.007

[11] Fonseca C. P., Neves S.: Electrochemical properties of a biodegradable polymer electrolyte applied to a rechargeable lithium battery. Journal of Power Sources, **159**, 712–716 (2006).
DOI: 10.1016/j.jpowsour.2005.10.095

[12] Fonseca C. P., Cavalcante Jr. F., Amaral F. A., Zani Souza C. A., Neves S.: Thermal and conduction properties of a PCL-biodegradable gel polymer electrolyte with $LiClO_4$, LiF_3CSO_3, and $LiBF_4$ salts. International Journal of Electrochemical Science, **2**, 52–63 (2007).

[13] Ng B. C., Wong H. Y., Chew K. W., Osman Z.: Development and characterization of poly-ε-caprolactone-based polymer electrolyte for lithium rechargeable battery. International Journal of Electrochemical Science, **6**, 4355–4364 (2011).

[14] Mikolajczak C., Kahn M., White K., Long R. T.: Lithium-ion batteries hazard and use assessment. Final Report 1100034.000 A0F0 0711 CM01. Fire Protection Research Foundation, Massachusetts (2011).

[15] Kumar G. G., Sampath S.: Electrochemical and spectroscopic investigations of a gel polymer electrolyte of poly(methylmethacrylate) and zinc triflate. Solid State Ionics **176**, 773–780 (2005).
DOI: 10.1016/j.ssi.2004.11.007

[16] Xu J. J., Ye H., Huang J.: Novel zinc ion conducting polymer gel electrolytes based on ionic liquids. Electrochemistry Communications, **7**, 1309–1317 (2005).
DOI: 10.1016/j.elecom.2005.09.011

[17] Kumar G. G., Sampath S.: Electrochemical characterization of poly(vinylidenefluoride)-zinc triflate gel polymer electrolyte and its application in solid-state zinc batteries. Solid State Ionics, **160**, 289–300 (2003).
DOI: 10.1016/S0167-2738(03)00209-1

[18] Kumar G. G., Sampath S.: Spectroscopic characterization of a gel polymer electrolyte of zinc triflate and polyacrylonitrile. Polymer, **45**, 2889–2895 (2004).
DOI: 10.1016/j.polymer.2004.02.053

[19] Wu I-D., Chang F-C.: Determination of the interaction within polyester-based solid polymer electrolyte using FTIR spectroscopy. Polymer, **48**, 989–996 (2007).
DOI: 10.1016/j.polymer.2006.12.045

[20] Gejji S. P., Hermansson K., Lindgren J.: Ab initio vibrational frequencies of the triflate ion, (CF_3SO_3)–. The Journal of Physical Chemistry, **97**, 3712–3715 (1993).
DOI: 10.1021/j100117a014

[21] Frech R., Chintapalli S., Bruce P. G., Vincent C. A.: Structure of an amorphous polymer electrolyte, poly (ethyleneoxide)$_3$:$LiCF_3SO_3$. Chemical Communications, **1997**, 157–158 (1997).
DOI: 10.1039/A606264D

[22] Macdonald J. R., Johnson W. B.: Impedance spectroscopy: Theory, experiment, and applications. Wiley, New Jersey (2005).

[23] Mark J. E.: Polymer data handbook. Oxford University Press, New York (1999).

[24] Hyun J.: A new approach to characterize crystallinity by observing the mobility of plasma treated polymer surfaces. Polymer, **42**, 6473–6477 (2001).
DOI: 10.1016/S0032-3861(01)00116-1

[25] Bhattacharya S. N., Kamal M. R., Gupta R. K.: Polymeric nanocomposites: Theory and practice. Hanser, Munich (2008).

[26] Avella M., Errico M. E., Laurienzo P., Martuscelli E., Raimo M., Rimedio R.: Preparation and characterisation of compatibilised polycaprolactone/starch composites. Polymer, **41**, 3875–3881 (2000).
DOI: 10.1016/S0032-3861(99)00663-1

[27] Woo H. J., Majid S. R., Arof A. K.: Transference number and structural analysis of proton conducting polymer electrolyte based on poly(ε-caprolactone). Materials Research Innovations, **15**, s49–s54 (2011).
DOI: 10.1179/143307511X13031890747697

[28] Wright P. V.: Structure, morphology and thermal properties of crystalline complexes of poly(ethylene oxide) and alkali salts. in 'Polymer electrolyte reviews' (eds.: MacCallum J. R., Vincent C. A.) Elsevier, New York, Vol 2, 61–119 (1989).

[29] Scrosati B.: Electrode kinetics and electrochemical cells. in 'Polymer electrolyte reviews' (eds.: MacCallum J. R., Vincent C. A.) Elsevier, New York, Vol 1, 315–345 (1987).

[30] Song M-K., Kim Y-T., Kim Y. T., Cho B. W., Popov B. N., Rhee H-W.: Thermally stable gel polymer electrolytes. Journal of the Electrochemical Society, **150**, 439–444 (2003).
DOI: 10.1149/1.1556592

[31] Rogulski Z., Chotkowski M., Czerwinski A.: New generation of the zinc-manganese dioxide cell. Journal of New Materials for Electrochemical Systems, **9**, 333–338 (2006).

[32] Kumar G. G., Munichandraiah N.: Reversibility of Mg/Mg^{2+} couple in a gel polymer electrolyte. Electrochimica Acta, **44**, 2663–2666 (1999).
DOI: 10.1016/S0013-4686(98)00388-0